


## Finite frequency noise in a chiral Luttinger liquid coupled to phonons

Edvin G. Idrisov 

*Physics and Materials Science Research Unit, University of Luxembourg, L-1511 Luxembourg, Luxembourg*



(Received 30 April 2019; revised manuscript received 19 August 2019; published 21 October 2019)

We study transport between quantum Hall edge states at filling factor  $\nu = 1$  in the presence of electron-acoustic-phonon coupling. After a Bogoliubov-Valatin transformation, the low-energy spectrum of interacting electron-phonon system is presented. The electron-phonon interaction splits the spectrum into charged and neutral “downstream” and neutral “upstream” modes with different velocities. In the regimes of dc and periodic ac biases the tunneling current and nonequilibrium finite frequency nonsymmetrized noise are calculated perturbatively in tunneling coupling of the quantum point contact. We show that the presence of electron-phonon interaction strongly modifies noise and current relations compared to the free-fermion case.

DOI: [10.1103/PhysRevB.100.155422](https://doi.org/10.1103/PhysRevB.100.155422)

### I. INTRODUCTION

Electron-phonon interactions play an important role in three-dimensional solid-state physics, for instance, to explain superconductivity [1,2]. However, intense theoretical and experimental investigations have indicated that the static and dynamical properties of electrons in one-dimensional (1D) Luttinger liquids are expected to be strongly modified by the presence of electron-phonon interaction as well [3–13]. Indeed, Martin and colleagues [3,4], using a Luttinger liquid description, calculated the exponents of correlation functions and discussed their remarkable sensitivity to the Wentzel-Bardeen [14,15] singularity induced by the presence of acoustic phonons. Next, in Ref. [8] the transport in a suspended metallic single-wall carbon nanotube in the presence of strong electron-phonon interaction was investigated. It was shown that the differential conductance as a function of applied bias voltage demonstrates three distinct types of phonon-assisted peaks. These peaks are best observed when the system is in the vicinity of the Wentzel-Bardeen singularity. Later, using functional bosonization, Galda *et al.* [10–12] studied the impact of electron-phonon coupling on electron transport through a Luttinger liquid with an embedded scatterer. They investigated the directions of renormalization group flows which can be changed by varying the ratio of Fermi (electron-electron interaction strength) to sound (electron phonon strength) velocities. A phase diagram was revealed with up to three fixed points: an unstable one with a finite value of conductance and two stable ones, corresponding to an ideal metal or insulator. The existence of only two stable fixed points (the ideal metal or the ideal insulator) is guaranteed by the duality in a multichannel Luttinger liquid [16,17].

Concurrently, the transport properties of electrons in chiral 1D systems has been a subject of intensive theoretical and experimental studies for a long time as well [18]. The experimental investigation of such systems was made possible mostly as a result of the discovery of integer and fractional quantum Hall (QH) effects in a two-dimensional electron gas (2DEG) [19,20]. The chiral electron states appearing at the edge of a 2DEG may be considered a quantum analog of

classical skipping orbits. Electrons in these 1D chiral states are basically similar to photons: they propagate only in one direction, and there is no intrinsic backscattering along the QH edge in the case of identical chiralities. However, electrons satisfy Fermi-Dirac statistics and are strongly interacting particles.

In order to study chiral 1D edge excitations a low-energy effective theory was introduced by Wen [21]. The key idea behind this approach is to represent the fermionic field in terms of collective bosonic fields. This so-called bosonization technique allows one to diagonalize the edge Hamiltonian of interacting 1D electrons with a linear spectrum and calculate any equilibrium correlation functions. Wen’s bosonization technique triggered better theoretical understanding of transport properties of 1D chiral systems and explains a lot of experimental findings [22]. Particularly, the tunneling current, nonequilibrium symmetric quantum noise between chiral fractional QH edge states and the photoassisted current, and shot noise in the fractional QH effect were studied [23–27]. It was shown that the differential conductance is nonzero at finite temperature and manifests a power-law behavior,  $G \propto T^{2(g-1)}$ , where  $T$  is the temperature and  $g$  depends on the filling factor of the fractional QH state. The exponent  $g = \nu$ , or  $g = 1/\nu$ , depending on the geometry of the tunneling constriction, where  $\nu$  is the filling factor. At zero temperature it has been demonstrated that the tunneling current has the form  $I \propto \mu^{2g-1}$ , where  $\mu$  is an applied dc bias. In the lowest order of tunneling coupling at zero temperature it was shown that the symmetric nonequilibrium noise is given by  $S(\omega) \propto \sum_{\sigma=\mp} |\omega + \sigma\omega_0|^{2g-1}$ , where  $\omega_0 = e^*\mu/\hbar$  is the Josephson frequency [28] of the electron or quasiparticle and  $e^*$  is the effective charge of the tunneling quasiparticle. Thus, an algebraic singularity is present at the Josephson frequency, which depends on charge  $e^*$ . At finite temperature it was shown that the ratio between nonequilibrium and equilibrium Johnson-Nyquist noises does not depend on the parameter  $g$  and has the familiar form  $S(\omega, \mu)/S(\omega, 0) = (e^*\mu/2T) \coth(e^*\mu/2T)$ .

In Ref. [29] it was already shown that the chiral QH edge state at filling factor  $\nu = 1$  is not a Fermi liquid in the presence of electron-phonon interaction. As a consequence the electron

correlation function is modified. Particularly, it was demonstrated that the ac conductance of the chiral channel exhibits resonances at longitudinal wave vectors  $q$  and frequencies  $\omega$  related by  $q = \omega/v_1$ ,  $q = \omega/v_2$ , and  $q = -\omega/v_3$ , where  $v_1$ ,  $v_2$ ,  $v_3$  are renormalized Fermi and sound velocities. However, it was claimed that the dc Hall conductance is not modified by electron-phonon interaction and is given by  $G_H = e^2/2\pi\hbar$ . Moreover, we would like to mention that according to the Wiedemann-Franz law [30,31], the thermal Hall conductance is not changed as well, namely,  $K_H = TG_H L_0$ , where  $T$  is the temperature and  $L_0 = (\pi^3/3)(k_B/e)^2$  is the free-fermion Lorenz number (see Appendix C).

Motivated by the previous progress in Ref. [29], we take a further step to investigate the noise properties of the tunneling current between two  $\nu = 1$  edge states in the presence of strong electron-acoustic phonon interaction. Such a system may be realized in conventional electron optics experiments [32] and also in bilayer systems with a total filling factor equal to 2 [18]. At filling factor  $\nu = 1$  we deal with a 1D chiral free-fermion system and no electron-electron interaction influences on tunneling current and noise. Therefore, any modifications will arise due to electron-phonon interactions. We expect that one may investigate this experimentally as in the works by Milliken *et al.* [33], where the authors measured the temperature dependence of the tunneling current between edge states with electron-phonon interaction.

The rest of the paper is organized as follows. In Sec. II, we introduce the model of the system, starting with the Hamiltonian of all the constituting parts and the bosonization prescription, and provide a Bogoliubov-Valatin (BV) transformation in order to calculate exactly the correlation function. In Sec. III, we calculate perturbatively the tunneling current in the regime of dc bias. In Sec. IV, we calculate the finite frequency nonsymmetrized noise in the dc regime. Section V is devoted to the derivation of the tunneling current in the regime of periodic ac bias. The result for finite frequency nonsymmetrized noise under the external ac bias is given in Sec. VI. We present our conclusions and future perspectives in Sec. VII. Details of calculations and additional information are presented in the Appendixes. Throughout the paper, we set  $|e| = \hbar = k_B = 1$ .

## II. THEORETICAL MODEL

### A. QH edge coupled to phonons

We start by introducing the total Hamiltonian of the system of QH edge states at filling factor  $\nu = 1$  coupled to acoustic phonons. The relevant energy scales in the experiments with such systems are sufficiently small compared to the Fermi energy  $\epsilon_F$ , which suggests using the effective low-energy theory of QH edge states [23]. The advantage of this approach is that it allows us to take into account exactly the electron-electron and, particularly in our case, the strong electron-phonon interactions. According to the effective theory, edge states can be described as collective fluctuations of the charge density  $\hat{\rho}(x)$ . The charge density operator is expressed in terms of bosonic field  $\hat{\phi}(x)$ , namely,  $\hat{\rho}(x) = (1/2\pi)\partial_x\hat{\phi}(x)$ . The boson field  $\hat{\phi}(x)$  can be written in terms of boson creation and annihilation operators,  $\hat{a}_k^\dagger = \sqrt{L/2\pi k}\hat{\rho}_k$  and

$\hat{a}_k = \sqrt{L/2\pi k}\hat{\rho}_{-k}$ , which satisfy a standard commutation relation  $[\hat{a}_k, \hat{a}_{k'}^\dagger] = \delta_{kk'}$ , i.e.,

$$\hat{\phi}(x) = \hat{\phi}_0 + 2\pi\hat{\pi}_0x + \sum_{k>0} \sqrt{\frac{2\pi}{Lk}} [e^{ikx}\hat{a}_k + e^{-ikx}\hat{a}_k^\dagger], \quad (1)$$

where zero modes fulfill the canonical commutation relation  $[\hat{\pi}_0, \hat{\phi}_0] = i/L$  and  $L$  is the total size of the system. We consider the thermodynamic limit  $L \rightarrow +\infty$ ; consequently,  $L$  drops out in the final results.

The total Hamiltonian includes three terms:

$$\hat{H} = \hat{H}_0 + \hat{H}_{ph} + \hat{H}_{e-ph}. \quad (2)$$

Here the first term

$$\hat{H}_0 = \frac{v_F}{4\pi} \int dx [\partial_x \hat{\phi}(x)]^2 \quad (3)$$

is the free part of the total Hamiltonian, where  $v_F$  is the Fermi velocity.

The second term describes free phonons,

$$\hat{H}_{ph} = \frac{1}{2} \int dx \left[ \zeta v_s^2 (\partial_x \hat{d})^2 + \frac{1}{\zeta} \hat{\Pi}_d^2 \right], \quad (4)$$

where  $\hat{d}(x)$  is a phonon field operator,  $\hat{\Pi}_d(x)$  is the canonical conjugate to it,  $v_s$  is the sound velocity, and  $\zeta$  is the linear mass density of the crystal. The phonon field and its conjugate are given by the following sums of phonon creation and annihilation operators:

$$\begin{aligned} \hat{\Pi}_d(x) &= i \sum_k \sqrt{\frac{v_s \zeta |k|}{2L}} e^{ikx} (\hat{b}_k^\dagger - \hat{b}_{-k}), \\ \hat{d}(x) &= \sum_k \sqrt{\frac{1}{2L \zeta v_s |k|}} e^{ikx} (\hat{b}_k^\dagger + \hat{b}_{-k}). \end{aligned} \quad (5)$$

The third term takes into account the strong electron-phonon interaction

$$\hat{H}_{e-ph} = D \int dx \hat{\rho}(x) \partial_x \hat{d}(x), \quad (6)$$

where  $D = \sqrt{\pi \zeta v_s^3}$  is an electron-phonon coupling (deformation potential constant). Strictly speaking, phonons are not 1D, and one needs to take into account all phonon modes. This means that apart from the intraedge interaction with electrons, Eq. (6), phonons can mediate the interedge interaction. The latter can substantially change the physics of the QH edge state. However, here, according to Ref. [29], we assume that one normal mode of the phonons is along the QH edge. Next, for phonons with a wavelength much larger than the cross section of the edge strip, the perpendicular normal modes contribute as an overall constant in the adiabatic approximation and can be ignored.

For further consideration it is convenient to rewrite the total Hamiltonian in Eq. (2) in momentum representation

$$\begin{aligned} \hat{H} &= \sum_{k>0} v_F k \hat{a}_k^\dagger \hat{a}_k + \sum_{k>0} v_s k [\hat{b}_k^\dagger \hat{b}_k + \hat{b}_{-k}^\dagger \hat{b}_{-k}] \\ &+ \sum_{k>0} [v_c k (\hat{b}_k^\dagger + \hat{b}_{-k}) \hat{a}_k + \text{H.c.}], \end{aligned} \quad (7)$$

where  $v_c = D/\sqrt{\pi \zeta v_s}$  and we ignore zero modes as well. Typically, the sound velocity is much smaller than the Fermi

velocity. However, according to Ref. [29], it should be possible to see the effects of electron-phonon interactions in GaAs heterojunctions. For instance, at magnetic fields of the order of 5 T and 2D electron densities of the order of  $10^{15} \text{ m}^{-2}$ , the Fermi velocity might be of the order of the sound velocity  $v_s \sim 5 \times 10^3 \text{ m/s}$  [29,34].

The Hamiltonian in Eq. (2) gives a complete description of our system. We note that Hamiltonian  $\hat{H}$  is bilinear in boson creation and annihilation operators; thus, the dynamics associated with this Hamiltonian can be accounted for exactly by solving linear equations of motion. However, the solution of the equation of motion has an inconvenient and complex form. To overcome those difficulties, we use the alternative way below, applying the BV transformation to diagonalize the total Hamiltonian.

### B. Bogoliubov-Valatin transformation

Using the operator identity  $[\hat{a}\hat{b}, \hat{c}] = \hat{a}[\hat{b}, \hat{c}] + [\hat{a}, \hat{c}]\hat{b}$  for bosonic operators, the equations of motion can be derived from Eq. (7):

$$\frac{d}{dt} \begin{bmatrix} \hat{a}_k(t) \\ \hat{b}_k(t) \\ \hat{b}_{-k}^\dagger(t) \end{bmatrix} = -iv_s k A \begin{bmatrix} \hat{a}_k(t) \\ \hat{b}_k(t) \\ \hat{b}_{-k}^\dagger(t) \end{bmatrix}. \quad (8)$$

$$B = \begin{bmatrix} b_{11} & b_{12} & b_{13} \\ b_{21} & b_{22} & b_{23} \\ b_{31} & b_{32} & b_{33} \end{bmatrix} = \begin{bmatrix} \sqrt{\frac{(\lambda_1^2-1)^2}{(\lambda_1^2-1)^2+4\beta^2\lambda_1}} & \sqrt{\frac{(\lambda_2^2-1)^2}{(\lambda_2^2-1)^2+4\beta^2\lambda_2}} & \sqrt{\frac{(\lambda_3^2-1)^2}{-(\lambda_3^2-1)^2-4\beta^2\lambda_3}} \\ \frac{\beta}{\lambda_1-1} \sqrt{\frac{(\lambda_1^2-1)^2}{(\lambda_1^2-1)^2+4\beta^2\lambda_1}} & \frac{\beta}{\lambda_2-1} \sqrt{\frac{(\lambda_2^2-1)^2}{(\lambda_2^2-1)^2+4\beta^2\lambda_2}} & \frac{\beta}{\lambda_3-1} \sqrt{\frac{(\lambda_3^2-1)^2}{-(\lambda_3^2-1)^2-4\beta^2\lambda_3}} \\ \frac{-\beta}{\lambda_1+1} \sqrt{\frac{(\lambda_1^2-1)^2}{(\lambda_1^2-1)^2+4\beta^2\lambda_1}} & \frac{-\beta}{\lambda_2+1} \sqrt{\frac{(\lambda_2^2-1)^2}{(\lambda_2^2-1)^2+4\beta^2\lambda_2}} & \frac{-\beta}{\lambda_3+1} \sqrt{\frac{(\lambda_3^2-1)^2}{-(\lambda_3^2-1)^2-4\beta^2\lambda_3}} \end{bmatrix}, \quad (12)$$

where  $\lambda_1$ ,  $\lambda_2$ , and  $\lambda_3$  are real eigenvalues of Eq. (10). The straightforward algebra confirms that the BV matrix diagonalizes the initial total bosonic Hamiltonian (7). Namely, we get the following quadratic form (the nonessential constant term is omitted):

$$\hat{H} = \sum_{k>0} \epsilon_1 \hat{\alpha}_k^\dagger \hat{\alpha}_k + \sum_{k>0} \epsilon_2 \hat{\beta}_k^\dagger \hat{\beta}_k + \sum_{k>0} \epsilon_3 \hat{\gamma}_{-k}^\dagger \hat{\gamma}_{-k}, \quad (13)$$

where  $\epsilon_i = v_i k$ ,  $i = 1, 2, 3$ , and  $v_1 = \lambda_1 v_s > 0$ ,  $v_2 = \lambda_2 v_s > 0$ , and  $v_3 = -\lambda_3 v_s > 0$ . One can check that the relations  $\epsilon_1 + \epsilon_2 - \epsilon_3 = \epsilon_F$  and  $b_{11}^2 + b_{12}^2 - b_{13}^2 = 1$  are invariants of the BV transformation and the statistics of the system, i.e., commutation relations of boson operators, is preserved after the BV transformation. The renormalized spectrum is given in Figs. 2 and 3. From these figures we see that  $\epsilon_1$  and  $\epsilon_2$  are strongly modified by electron-phonon interactions in comparison to free plasmons, collective excitation of the QH edge and free phonons, and  $\epsilon_3$  is slightly changed from its initial value  $\epsilon_s$ . The elements of the first row of the BV transformation are given in Figs. 4–7.

According to the BV transformation the bosonic operator is expressed in terms of three independent bosonic terms [29], namely,

$$\hat{a}_k = b_{11} \hat{\alpha}_k + b_{12} \hat{\beta}_k + b_{13} \hat{\gamma}_{-k}^\dagger. \quad (14)$$

This equation is the main result of this section. It will be used in the next section to calculate the two-point correlation function.

Here the dimensionless  $3 \times 3$  matrix has the following form:

$$A = \begin{bmatrix} \alpha & \beta & \beta \\ \beta & 1 & 0 \\ -\beta & 0 & -1 \end{bmatrix}, \quad (9)$$

where  $\alpha = v_F/v_s$  and  $\beta = v_c/v_s$ . We call it a dynamical matrix.

Next, according to Ref. [35], the Hamiltonian of bosons in Eq. (7) is BV diagonalizable if its dynamical matrix is physically diagonalizable (stable theory). The dynamical matrix is said to be stable if it is diagonalizable, and all its eigenvalues are real. Therefore, we write the characteristic equation to find the eigenvalues,

$$\lambda^3 - \alpha\lambda^2 - \lambda + \chi = 0, \quad (10)$$

where we introduced the notation  $\chi = \alpha - 2\beta^2$ . To have three distinct real eigenvalues the coefficients of the characteristic cubic equation must satisfy the inequality (see Fig. 1)

$$g(\alpha, \beta) = 18\alpha\chi + 4\alpha^3\chi + (\alpha^2 + 4) - 27\chi^2 > 0. \quad (11)$$

The eigenvalues of dynamical matrix (9) are provided in Appendix A. Using the ideas of Ref. [35], one can construct the BV transformation matrix,

### C. Correlation function

The important quantity which allows us to describe the transport properties of the system under consideration is the equilibrium two-point correlation function. It is defined as  $G(x_1, t_1; x_2, t_2) = \langle \hat{\psi}^\dagger(x_1, t_1) \hat{\psi}(x_2, t_2) \rangle$ , where, according to the bosonization technique, the fermionic field is given by  $\hat{\psi}(x) \propto \exp[i\hat{\phi}(x)]$ , where we omit the ultraviolet cutoff prefactor. The average is taken with respect to the equilibrium density matrix  $\hat{\rho}_0 \propto \exp[(\hat{H}_0 + \hat{H}_{ph})/T]$ , and  $T$  is temperature.

Next, using the expansion of bosonic fields in terms of collective modes in Eq. (1) and the BV transformation in Eqs. (12)–(14), we finally arrive at the following result for the fermion correlation function [29] (see Appendix B):

$$G(x_1, t_1; x_2, t_2) \propto \left[ \frac{i\eta}{x_1 - x_2 - v_1(t_1 - t_2) + i\eta} \right]^{b_{11}^2} \times \left[ \frac{i\eta}{x_1 - x_2 - v_2(t_1 - t_2) + i\eta} \right]^{b_{12}^2} \times \left[ \frac{-i\eta}{x_1 - x_2 + v_3(t_1 - t_2) - i\eta} \right]^{b_{13}^2}, \quad (15)$$

where  $\eta = a/2\pi$  and  $a$  is an ultraviolet cutoff.

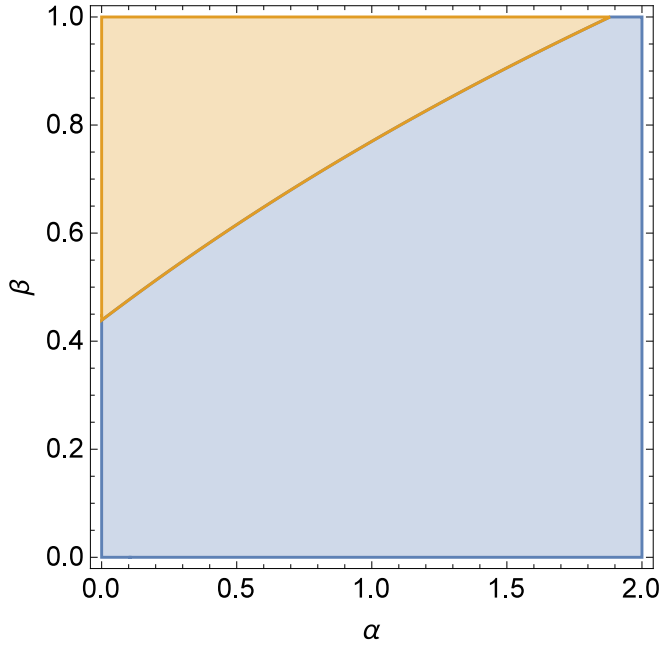


FIG. 1. The condition of validation of the BV transformation. The light orange region satisfies the inequality  $g(\alpha, \beta) < 0$ , and the light blue region is given by  $g(\alpha, \beta) > 0$ . The BV transformation is valid in the light blue region.

The free-fermion two-point correlation function for the right-moving mode is proportional to  $\propto i\eta/[x_1 - x_2 - v_F(t_1 - t_2) + i\eta]$ . Here we see that the electron-phonon interaction changes the correlation function sufficiently compared to the free-fermion one.

The finite temperature correlation function is obtained by applying a conformal transformation [36]. To apply the conformal transformation we go to Euclidean time  $-i\tau_E = t_1 - t_2 - (x_1 - x_2)/v$  and then set  $v\tau_E \rightarrow (v/2\pi T)\arctan(2\pi T\tau_E)$ . It follows that

$$G(x_1, t_1; x_2, t_2) \propto \left[ \frac{iaT/2v_1}{\sinh\left\{\frac{\pi T}{v_1}[x_1 - x_2 - v_\alpha(t_1 - t_2)] + i\eta\right\}} \right]^{b_{11}^2}$$

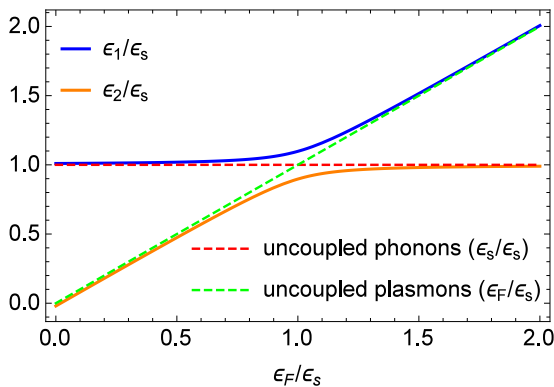


FIG. 2. The renormalized spectrum of  $\epsilon_1/\epsilon_s$  and  $\epsilon_2/\epsilon_s$  as a function of renormalized Fermi energy  $\epsilon_F/\epsilon_s$ . For comparison the spectrum of the uncoupled phonon and plasmon system is shown as well. We set  $\beta = 0.1$ .

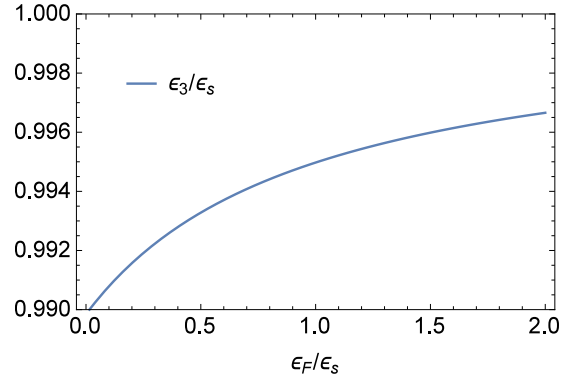


FIG. 3. The renormalized spectrum of  $\epsilon_3/\epsilon_s$  as a function of renormalized Fermi energy  $\epsilon_F/\epsilon_s$ . We set  $\beta = 0.1$ .

$$\times \left[ \frac{iaT/2v_2}{\sinh\left\{\frac{\pi T}{v_2}[x_1 - x_2 - v_2(t_1 - t_2)] + i\eta\right\}} \right]^{b_{12}^2} \times \left[ \frac{-iaT/2v_3}{\sinh\left\{\frac{\pi T}{v_3}[x_1 - x_2 + v_3(t_1 - t_2)] - i\eta\right\}} \right]^{b_{13}^2}. \quad (16)$$

As one can mention, the correlation function splits into three independent correlation functions with different velocities. Two of them with velocities  $v_1$  and  $v_2$  correspond to “down-stream” modes. One of these modes,  $v_1$ , carries a charge. The third correlation function is related to the “upstream” mode and travels on the opposite side with respect to the right-moving downstream modes. In the following sections we use these correlators to derive the tunneling current and noise perturbatively in the tunneling coupling.

### III. TUNNELING CURRENT IN THE dc REGIME

The electron-phonon interaction is taken into account exactly; therefore, the tunneling has to be considered perturbatively. The tunneling (backscattering) Hamiltonian of electrons at the quantum point contact (QPC) located at point  $x$  is given by

$$\hat{H}_T = \hat{A} + \hat{A}^\dagger, \quad \hat{A} = \tau \hat{\psi}_d^\dagger(x) \hat{\psi}_u(x), \quad (17)$$

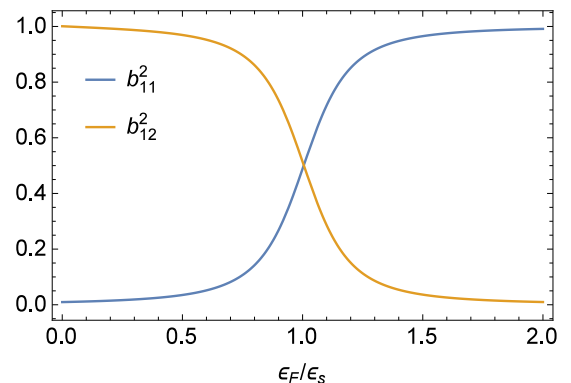


FIG. 4. The squares of the first two matrix elements of the BV transformation as a function of renormalized Fermi energy  $\epsilon_F/\epsilon_s$  [see Eq. (12)]. We set  $\beta = 0.1$ .

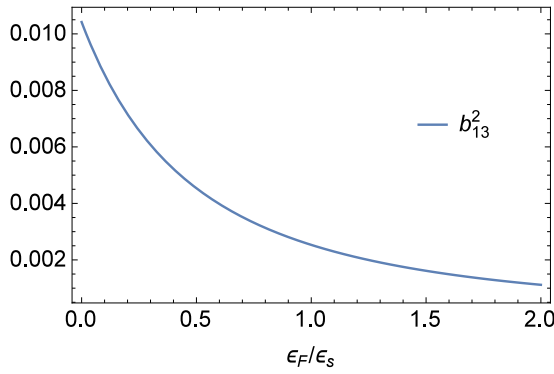


FIG. 5. The square of the third matrix element of the BV transformation as a function of renormalized Fermi energy  $\epsilon_F/\epsilon_s$  [see Eq. (12)]. We set  $\beta = 0.1$ .

where  $\tau$  (generally a complex number) is the tunneling coupling constants and  $\hat{\psi}_i(x)$ ,  $i = u, d$ , is an electron annihilation operator [37,38] in the  $i$ th channel. The vertex operator  $\hat{A}$  in Eq. (17) mixes the up ( $u$ ) and down ( $d$ ) channels and transfers electrons from one channel to another (see Fig. 8). We introduce the tunneling current operator  $\hat{J} = \hat{N}_d = i[\hat{H}_T, \hat{N}_d]$ , where  $\hat{N}_d = \int dx \hat{\psi}_d^\dagger(x) \hat{\psi}_d(x)$  is the number of electrons in the down channel. After simple algebra we obtain the tunneling current operator

$$\hat{J} = i(\hat{A}^\dagger - \hat{A}). \quad (18)$$

In the interaction representation the average current is given by the expression

$$I = \langle \hat{U}^\dagger(t, -\infty) \hat{J}(t) \hat{U}(t, -\infty) \rangle, \quad (19)$$

where the average is taken with respect to the dc biased ground state in QH edges and free phonons and at the lowest order of tunneling coupling the evolution operator is given by

$$\hat{U}(t_1, t_2) \approx 1 - i \int_{t_2}^{t_1} dt \hat{H}_T(t). \quad (20)$$

We evaluate the average current by perturbatively expanding the evolution operator to the lowest order in the tunneling amplitude. It is clear that the average tunneling current can be written as a commutator of vertex operators; namely, one

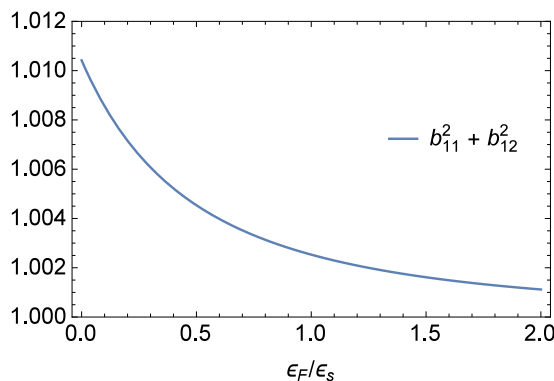


FIG. 6. The sum of squares of the first two BV matrix elements [see Eq. (12)]. We set  $\beta = 0.1$ . Note that the sum is not equal to 1.

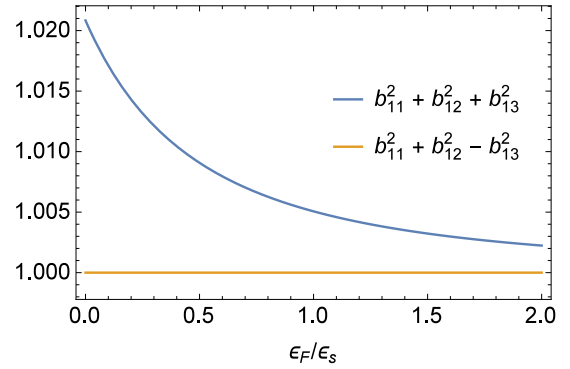


FIG. 7. The relations between the first row elements of the BV matrix in Eq. (12). We set  $\beta = 0.1$ .

obtains

$$I = \int dt \langle [\hat{A}^\dagger(t), \hat{A}(0)] \rangle. \quad (21)$$

The perturbative result is valid as long as the tunneling current  $I$  is small compared to the Hall current  $I_H = G_H \mu$ , where  $\mu$  is a dc bias applied between upper and lower chiral channels (see Fig. 8). In our model there is no interaction between upper and lower channels; that is, they are independent, and therefore, the correlation functions in Eq. (21) split into the product of two single-particle correlators, namely,

$$I = |\tau|^2 \int dt e^{i\mu t} [\langle \hat{\psi}_u^\dagger(t) \hat{\psi}_u(0) \rangle \langle \hat{\psi}_d(t) \hat{\psi}_d^\dagger(0) \rangle - \langle \hat{\psi}_d^\dagger(0) \hat{\psi}_d(t) \rangle \langle \hat{\psi}_u(0) \hat{\psi}_u^\dagger(t) \rangle], \quad (22)$$

where, for definiteness, we set  $x = 0$  and the average now is taken with respect to the equilibrium density matrix  $\hat{\rho}_0$  from Sec. II. Next, without loss of generality we consider the case of positive bias  $\mu > 0$ . The sign of the bias  $\mu$  simply determines the direction of the current. Substituting the correlation functions from Eq. (15) into Eq. (22) and employing the integral

$$\lim_{\eta \rightarrow +0} \int \frac{e^{\eta + iy}}{(\eta + iy)^b} dy = \frac{2\pi}{\Gamma[b]}, \quad (23)$$

where  $y = \mu t$  is a dimensionless variable of integration, we obtain the expression for tunneling current at zero tempera-

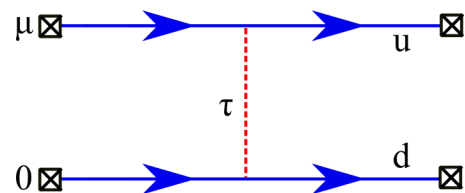


FIG. 8. Schematic representation of the setup: A QPC (dashed red line) with tunneling amplitude  $\tau$  connects up ( $u$ ) and down ( $d$ ) chiral edge channels of integer QH at filling factor  $\nu = 1$ . Each channel is coupled to acoustic phonons. The bias  $\mu$  is applied to the upper incoming edge channel, while the down edge channel is grounded.

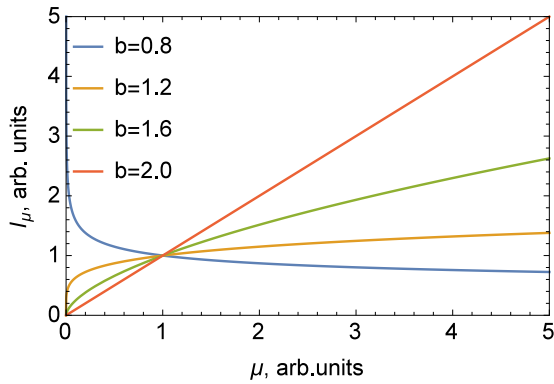


FIG. 9. The tunneling current  $I_\mu$  versus applied dc voltage  $\mu$  at zero temperature for different even values of  $b$  [see Eq. (24)].

ture:

$$I_\mu \propto \mathcal{D} |\tau|^2 \frac{2\pi}{\Gamma[b]} \mu^{b-1}, \quad (24)$$

where  $\mathcal{D} = (2\pi v_1)^{-2b_{11}^2} (2\pi v_2)^{-2b_{12}^2} (2\pi v_3)^{-2b_{13}^2}$  is the renormalized density of states in the presence of electron-phonon interaction,  $b = 2(b_{11}^2 + b_{12}^2 + b_{13}^2)$ ,  $\Gamma[b]$  is the Euler gamma function, and we omit the prefactor which depends on the ultraviolet cutoff. The dependence of the tunneling current on applied dc bias is presented in Figs. 9 and 10. It is a monotonic function.

For the case of finite temperature an analytical continuation on the complex plane is applied to Eq. (22). Then shifting the integration variable  $\pi T t = u + i\pi/2$  (this does not affect the singularities of integrand) and using the integral

$$\lim_{\eta \rightarrow +0} \int \frac{e^{i\frac{\mu}{\pi T} u}}{\cosh^b[u + i\eta]} du = 2^{b-1} \frac{|\Gamma[\frac{1}{2}(b + i\frac{\mu}{\pi T})]|^2}{\Gamma[b]}, \quad (25)$$

we get the final result for the tunneling current,

$$I \propto 2\mathcal{D} |\tau|^2 (2\pi T)^b \sinh\left(\frac{\mu}{2T}\right) \frac{|\Gamma[\frac{1}{2}(b + i\frac{\mu}{\pi T})]|^2}{2\pi T \Gamma[b]}. \quad (26)$$

In the noninteracting free-fermion case at  $b = 2$ , the current is given by the well-known Landauer-Buttiker formula  $I = |\tau|^2 \mu / 2\pi v_F$ , and the QPC is in the Ohmic regime. However, a non-Ohmic behavior could be observed for the non-

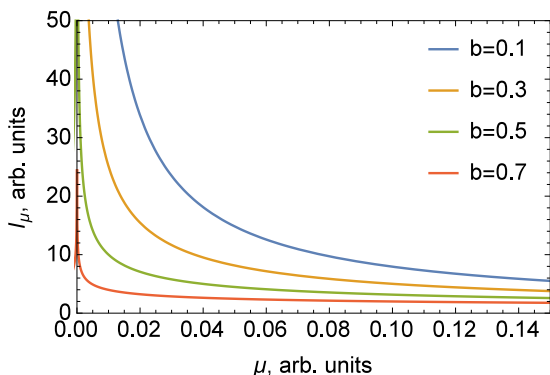


FIG. 10. The tunneling current  $I_\mu$  versus applied dc voltage  $\mu$  at zero temperature for different odd values of  $b$  [see Eq. (24)].

Fermi liquid. Namely, at high temperatures from Eq. (26) we obtain

$$I \propto T^{b-2} \mu, \quad \mu/T \ll 1, \quad (27)$$

which demonstrates an Ohmic behavior, and at low temperatures we get the expression

$$I \propto \mu^{b-1}, \quad \mu/T \gg 1, \quad (28)$$

with non-Ohmic behavior, specific for a non-Fermi liquid.

Next, apart from the current or conductance it is useful to measure the time-dependent fluctuations of tunneling current, noise. For instance, it is known that measuring shot noise allows direct access to fractional charges of Laughlin quasiparticles [39]. The calculation of noise is the subject of the next sections.

#### IV. FINITE AND ZERO-FREQUENCY NOISE IN THE dc REGIME

##### A. Finite frequency noise

Experimentally, the measured spectral noise density of current fluctuations strongly depends on how the detector operates [40]. We consider the finite frequency nonsymmetrized noise. In the absence of time-dependent external fields the correlation function in Eqs. (15) and (16) depends on the time difference. This is true as well for finite frequency noise defined as

$$S(\omega) = \int dt e^{i\omega t} \langle \delta \hat{J}(t) \delta \hat{J}(0) \rangle, \quad (29)$$

where the average is taken with respect to the dc biased ground state in QH edges and free phonons as in Eq. (21) and  $\delta \hat{J}(t) = \hat{J}(t) - \langle \hat{J}(t) \rangle$ . This has become a measurable quantity in recent experiments [41]. We evaluate Eq. (29) perturbatively in the lowest order of tunneling coupling and get the following expression for finite frequency nonsymmetrized noise in terms of vertex operators, defined in Eq. (17), namely,

$$S(\omega) = \int dt e^{i\omega t} [\langle \hat{A}^\dagger(t) \hat{A}(0) \rangle + \langle \hat{A}(t) \hat{A}^\dagger(0) \rangle]. \quad (30)$$

One can mention that to obtain the symmetrized noise one needs to simply construct an even function of nonsymmetrized noise, i.e.,  $[S(\omega) + S(-\omega)]/2$ .

Evaluating Eq. (30) at zero temperature, we obtain the result for finite frequency nonsymmetrized noise:

$$S(\omega) \propto \mathcal{D} |\tau|^2 \frac{2\pi}{\Gamma[b]} \sum_{\sigma=\mp} |\omega + \sigma\mu|^{b-1} \theta(\omega + \sigma\mu), \quad (31)$$

where  $\theta(x)$  is the Heaviside function. The normalized finite frequency nonsymmetrized noise is plotted in Fig. 11. From Eq. (31) one can notice that at  $\omega \ll \mu$ , we obtain  $S(\omega) \propto I_\mu$ , which is the classical shot noise result of the next section. As expected, it does depend on the interaction parameter  $b$ . Note that at  $\omega = \mp\mu$  there are knife-edged singularities in finite frequency noise. In the case of a noninteracting fermionic liquid at  $b = 2$  these singularities are caused by the Pauli exclusion principle [28].

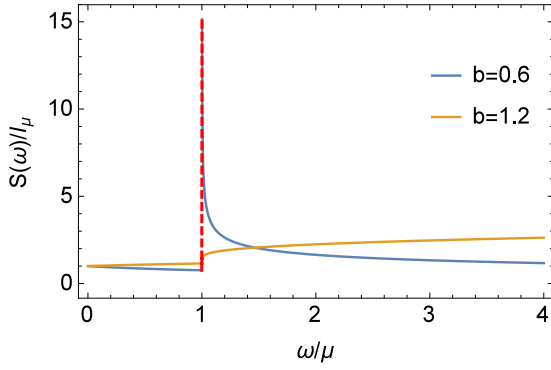


FIG. 11. The normalized nonsymmetrized finite frequency noise  $S(\omega)/I_\mu$  is plotted versus the dimensionless frequency  $\omega/\mu > 0$  (emission noise) at zero temperature and fixed dc bias  $\mu > 0$  [see Eq. (31)]. We set  $b = 0.6$  and  $b = 1.2$ .

For finite temperatures we substitute the correlation function from Eq. (16) into Eq. (30) and get

$$S(\omega) \propto \mathcal{D}|\tau|^2 (2\pi T)^b \sum_{\sigma=\mp} \frac{\exp\left(\frac{\omega+\sigma\mu}{2T}\right) \left| \Gamma\left[\frac{1}{2}(b + i\frac{\omega+\sigma\mu}{\pi T})\right] \right|^2}{2\pi T \Gamma[b]}. \quad (32)$$

Away from singularities at  $|\omega \mp \mu|/2T \gg 1$  we recover Eq. (31). At zero frequency this result coincides with Eq. (34) in the next section.

### B. Zero-frequency noise

Experimentally, the zero-frequency spectral noise density is studied as well [39]. Moreover, in the limit of zero frequency the nonsymmetrized and symmetrized noises coincide. Unlike the tunneling current, the zero-frequency noise is given by the anticommutator of vertex operators

$$S(0) = \int dt \langle \{\hat{A}^\dagger(t), \hat{A}(0)\} \rangle. \quad (33)$$

A straightforward calculation similar to what we have done to evaluate the tunneling current in Eq. (26) gives

$$S(0)/I = \coth\left(\frac{\mu}{2T}\right), \quad (34)$$

where the tunneling current  $I$  is given by Eq. (26). This expression is independent of the interaction parameter  $b$ . The current fluctuations satisfy a classical (Poissonian) shot noise form. This is related to uncorrelated tunneling of electrons through a QPC. The result is identical to the case of non-interacting electrons in the Landauer-Buttiker approach and shows that the electron-phonon interaction is not important; thus, successive electrons tunnel infrequently.

### V. TUNNELING CURRENT IN THE ac REGIME

To investigate the time-dependent driven case, we split the voltage applied to the upper edge contact into the dc and ac parts, namely,

$$V(t) = \mu + \mu_1 \cos(\Omega t), \quad (35)$$

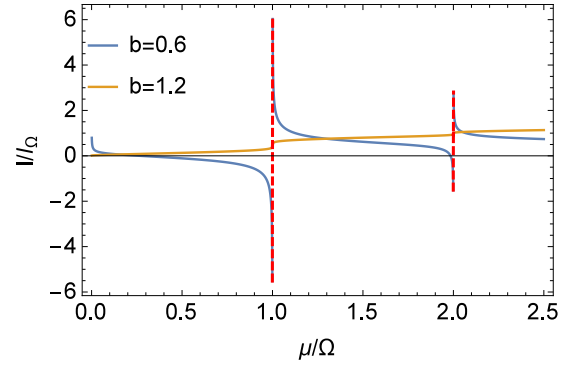


FIG. 12. The normalized tunneling current  $I/I_\Omega$  is plotted versus the dimensionless dc component of bias  $\mu/\Omega > 0$  at zero temperature and fixed  $\Omega > 0$  [see Eq. (40)]. Here we set  $b = 0.6$ ,  $b = 1.2$ ,  $\mu_1/\Omega = 2$ , and  $I_\Omega$  is given by Eq. (24) by simply replacing  $\mu$  by frequency  $\Omega$ .

where the ac part of  $V(t)$  averages to zero over one period  $\mathcal{T} = 2\pi/\Omega$  and the number of electrons per pulse is  $q = \mu/\Omega$ . One can consider more exotic shapes of the drive, such as a “train” of Lorentzian pulses ( $q = \mp 1, \mp 2, \dots$ ) in the context of levitons, the time-resolved minimal excitation states of a Fermi sea, recently detected in a 2DEG [42–45].

The time-averaged tunneling current between two edges in the case of ac voltage is given by the formula

$$I = 2\text{Re}[\mathcal{I}], \quad (36)$$

where the quantity in square brackets has the form

$$\mathcal{I} = \frac{1}{\mathcal{T}} \int_0^{\mathcal{T}} dt \int_{-\infty}^t dt' e^{i \int_{t'}^t V(\tilde{t}) d\tilde{t}} \langle [\hat{A}^\dagger(t), \hat{A}(t')] \rangle \quad (37)$$

and the average is taken with respect to the equilibrium density operator  $\rho_0$ . After substituting the exact form of vertex operators from Eq. (17) into Eq. (37) and taking into account that the up and down edges are independent, we get

$$\begin{aligned} \mathcal{I} = & \frac{1}{\mathcal{T}} \int_0^{\mathcal{T}} dt \int_{-\infty}^t dt' e^{i\mu(t-t')} e^{i\frac{\mu_1}{\Omega} [\sin(\Omega t) - \sin(\Omega t')]} \\ & \times [ \langle \hat{\psi}_u^\dagger(t) \hat{\psi}_u(t') \rangle \langle \hat{\psi}_d(t) \hat{\psi}_d^\dagger(t') \rangle \\ & - \langle \hat{\psi}_d^\dagger(t') \hat{\psi}_d(t) \rangle \langle \hat{\psi}_u(t') \hat{\psi}_u^\dagger(t) \rangle ]. \end{aligned} \quad (38)$$

Further progress in Eq. (38) is possible using the property of Bessel functions of the first kind,

$$\exp[i\xi \sin \varphi] = \sum_{n=-\infty}^{\infty} J_n(\xi) \exp[in\varphi], \quad (39)$$

where  $J_n(\xi)$  gives the Bessel function of the first kind and  $n$  is an integer.

Substituting Eqs. (15) and (39) into Eq. (38) and performing the time integration, we obtain the final result for the tunneling current at zero temperature,

$$I \propto \mathcal{D}|\tau|^2 \frac{2\pi}{\Gamma[b]} \sum_{n=-\infty}^{+\infty} J_n^2(\mu_1/\Omega) |\mu + n\Omega|^{b-1} \text{sgn}(\mu + n\Omega). \quad (40)$$

The normalized tunneling current is plotted in Fig. 12. At zero drive frequency,  $\mu_1/\Omega \rightarrow \infty$ , and positive dc bias  $\mu$  we recover the result in Eq. (24) in Sec. III. Because of the ac drive here we observe the singularities which strongly depend on the electron-phonon interaction parameter  $b$  and are related by a new energy scale, the drive frequency  $\Omega$ .

Identical steps as in the case of zero temperature bring us to the result for finite temperatures, namely,

$$I \propto 2\mathcal{D}|\tau|^2(2\pi T)^b \times \sum_{n=-\infty}^{+\infty} J_n^2(\mu_1/\Omega) \times \sinh\left(\frac{\mu + n\Omega}{2T}\right) \frac{|\Gamma[\frac{1}{2}(b + i\frac{\mu+n\Omega}{\pi T})]|^2}{2\pi T \Gamma[b]}. \quad (41)$$

At zero drive frequency and  $\mu_1/\Omega \rightarrow \infty$ , observing that  $\sum_{n=-\infty}^{\infty} J_n^2(\mu_1/\Omega) \rightarrow 1$ , we recover the result provided in Eq. (26) in Sec. III. We do not provide the plot at finite temperature, which is less interesting than the zero-temperature case. However, one has to mention that at high temperatures  $T \gtrsim \max\{\mu, \Omega\}$  the singularities are expected to smear out, and a thermal broadening appears. Consequently, the singularities are restored at low temperatures.

## VI. FINITE AND ZERO-FREQUENCY NOISE IN THE ac REGIME

### A. Finite frequency noise

The time-averaged phonon-assisted finite frequency nonsymmetrized noise is given by the Wigner transformation defined as

$$S(\omega) = \frac{1}{\mathcal{T}} \int_0^{\mathcal{T}} d\tau \int d\tau' S\left(\tau + \frac{\tau'}{2}, \tau - \frac{\tau'}{2}\right) e^{i\omega\tau'}, \quad (42)$$

where we introduced the ‘‘center of mass’’  $\tau = (t + t')/2$  and ‘‘relative’’  $\tau' = t - t'$  time coordinates. The integrand is given by the current fluctuation correlator in the time domain, namely,  $S(t, t') = \langle \delta\hat{J}(t)\delta\hat{J}(t') \rangle$ , with  $\delta\hat{J}(t) = \hat{J}(t) - \langle \hat{J}(t) \rangle$ , where the average is taken with respect to the ground state of QH edges with free phonons. Equation (42) is nothing but the Fourier transform of  $S(t, t')$  in terms of the relative time coordinate  $\tau'$ .

The straightforward calculations give the following result for the zero-temperature case:

$$S(\omega) \propto \mathcal{D}|\tau|^2 \frac{2\pi}{\Gamma[b]} \sum_{n=-\infty}^{+\infty} \sum_{\sigma=\mp} J_n^2(\mu_1/\Omega) \times |\omega + \sigma(\mu + n\Omega)|^{b-1} \theta[\omega + \sigma(\mu + n\Omega)]. \quad (43)$$

The normalized finite frequency nonsymmetrized noise at zero temperature is plotted in Fig. 13.

At finite temperature we get the following result for finite frequency nonsymmetrized noise:

$$S(\omega) \propto \mathcal{D}|\tau|^2 (2\pi T)^b \sum_{n=-\infty}^{+\infty} \sum_{\sigma=\mp} J_n^2(\mu_1/\Omega) \times \exp\left[\frac{\omega + \sigma(\mu + n\Omega)}{2T}\right] \frac{|\Gamma[\frac{1}{2}(b + i\frac{\omega + \sigma(\mu + n\Omega)}{\pi T})]|^2}{2\pi T \Gamma[b]}. \quad (44)$$

At zero frequency we recover the result in the next section.

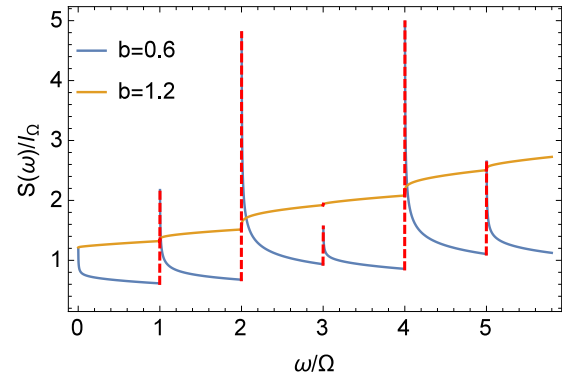


FIG. 13. The normalized unsymmetrized finite frequency noise  $S(\omega)/I_0$  is plotted versus the dimensionless frequency  $\omega/\Omega > 0$  (emission noise) at zero temperature and fixed  $\mu > 0$  and  $\Omega > 0$  [see Eq. (43)]. Here we set  $b = 0.6$ ,  $b = 1.2$ ,  $\mu_1/\Omega = 2$ ,  $\mu/\Omega = 3$ , and  $I_0$  is given by Eq. (24) by simply replacing  $\mu$  by frequency  $\Omega$ .

### B. Zero-frequency noise

The time-averaged zero-frequency nonsymmetrized noise is obtained from Eq. (42) and is given by the following anticommutator of vertex operators:

$$S(0) = \frac{1}{\mathcal{T}} \int_0^{\mathcal{T}} dt \int dt' e^{iJ_t^i V(\vec{r})dt'} \langle \{\hat{A}^\dagger(t + t'/2), \hat{A}(t - t'/2)\} \rangle. \quad (45)$$

At zero temperature and after the time integration in Eq. (45) we obtain the following expression for zero-frequency noise:

$$S(0) \propto \mathcal{D}|\tau|^2 \frac{2\pi}{\Gamma[b]} \sum_{n=-\infty}^{\infty} J_n^2(\mu_1/\Omega) |\mu + n\Omega|^{b-1}. \quad (46)$$

This result coincides with Eq. (43) for finite frequency noise at zero frequency. The normalized zero-frequency noise at zero temperature is plotted in Fig. 14.

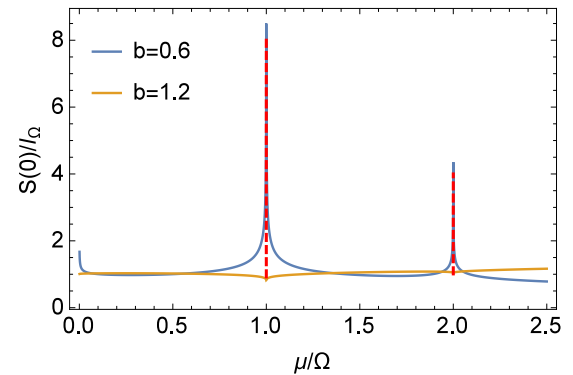


FIG. 14. The normalized unsymmetrized zero-frequency noise  $S(0)/I_0$  is plotted versus the dimensionless dc component of bias  $\mu/\Omega > 0$  at zero temperature and fixed  $\Omega > 0$  [see Eq. (46)]. Here we set  $b = 0.6$ ,  $b = 1.2$ ,  $\mu_1/\Omega = 2$ , and  $I_0$  is given by Eq. (24) by simply replacing  $\mu$  by frequency  $\Omega$ .



For finite temperature the straightforward calculation of the integral over the time variable results in

$$S(0) \propto 2D|\tau|^2(2\pi T)^b \sum_{n=-\infty}^{+\infty} J_n^2(\mu_1/\Omega) \times \cosh\left(\frac{\mu + n\Omega}{2T}\right) \frac{|\Gamma[\frac{1}{2}(b + i\frac{\mu+n\Omega}{\pi T})]|^2}{2\pi T \Gamma[b]}. \quad (47)$$

Here we can also mention that the result for finite frequency noise given by Eq. (44) at  $\omega \rightarrow +0$  transforms into Eq. (47).

## VII. CONCLUSION

In this paper we have studied the impact of strong electron-acoustic-phonon interaction on QH edge state transport. We have discussed the case of filling factor  $\nu = 1$ ; thus, no electron-electron interaction influences transport properties. Using Wen's effective low-energy theory of QH edge states and applying a BV transformation, we were able to take into account the electron-phonon interaction exactly. It was demonstrated that the equilibrium two-point correlation function splits into three independent correlation functions with different velocities. Namely, two of them correspond to downstream modes, and the third one is related to the upstream mode, in agreement with Ref. [29]. The presence of electron-phonon interaction strongly modifies the equilibrium propagator; that is, it destroys the Fermi liquid behavior in comparison with noninteracting electrons. It was already shown that dc Hall conductance of a single-branch QH edge with electron-phonon interaction is not varied and is given by quantum conductance,  $G_H = e^2/h$  [29]. In this paper we state that according to the Wiedemann-Franz law, the thermal Hall conductance is not modified as well, namely,  $K_H = TG_H L_0$ , where  $L_0$  is the free-fermion Lorentz number (see Appendix C).

We studied the tunneling current for a QPC in the lowest order of tunneling coupling under dc and ac biases. Perturbative results were obtained for the arbitrary interaction parameter  $b$ , which depends on electron-phonon coupling and Fermi and sound velocities. We observed that at high temperatures  $\mu/T \ll 1$  the tunneling current is proportional to applied dc bias,  $I \propto T^{b-2}\mu$ , which is the manifestation of Ohmic behavior of the QPC. However, at low temperatures,  $\mu/T \gg 1$ , we got a non-Ohmic behavior,  $I \propto \mu^{b-1}$ , specific for a non-Fermi liquid. In contrast, in the case of ac drive at zero temperature we observed singularities in the tunneling current. These singularities strongly depend on the electron-phonon interaction parameter  $b$  and are related by a new energy scale, the drive frequency  $\Omega$ . One has to mention that at high temperatures  $T \gtrsim \max\{\mu, \Omega\}$  the singularities are expected to smear out and to reveal the thermal broadening. Consequently, at low temperatures the singularities are restored.

In addition to current we studied the nonequilibrium finite frequency nonsymmetrized noise of tunneling current in dc and ac regimes. Here the correlations caused by electron-phonon interaction are responsible for algebraic singularities,  $\omega = \mp\mu$ ,  $\omega = \mp(\mu + n\Omega)$  at zero temperature, which depend on  $b$ , the electron-phonon interaction parameter. In

the case of dc bias the ratio between shot noise and current is independent of  $b$  and has the form  $S(0)/I = \coth(\mu/2T)$ . Thus, the current fluctuations satisfy a classical (Poissonian) shot noise form. This is related to uncorrelated tunneling of electrons through the QPC. The result is identical to the case of noninteracting electrons in the Landauer-Buttiker approach. Finally, we would like to point out that Eqs. (40), (41), (46), and (47) can be combined into one expression, namely,  $\Lambda_{ac} = \sum_{n=-\infty}^{\infty} J_n^2(\mu_1/\Omega) \Lambda_{dc}(\mu + n\Omega)$ , where  $\Lambda_{dc}(\mu + n\Omega)$  is given by Eqs. (24), (26), and (34), respectively. This is a general formula which applies to transport quantities, such as current, heat current, and shot noise under ac bias [46].

In conclusion, we have shown that the presence of electron-phonon interaction strongly modifies the analytical structures of noise and current compared to the free-fermion case. As a future perspective, it is appropriate to investigate the tunneling current and noise in two-QPC and resonant-level QH systems with Laughlin states in the presence of electron-phonon interaction, the periodic train of Lorentzian voltage pulses in the context of levitonic physics [45].

## ACKNOWLEDGMENTS

We are grateful to S. Groenendijk for a careful and critical reading of the manuscript and T. L. Schmidt, T. Martin, and C. Glattli for fruitful discussions. We acknowledge financial support from the Fonds National de la Recherche Luxembourg under Grants ATTRACT 7556175 and INTER 11223315.

## APPENDIX A: EIGENVALUES OF THE CHARACTERISTIC EQUATION

In this Appendix we present the eigenvalues of Eq. (10) from the main text. The three distinct real eigenvalues of this cubic equation are given by

$$\lambda_{1,2} = \frac{1}{3} \left( \alpha - \frac{1 \pm i\sqrt{3}}{2} \frac{\xi_1}{\sqrt[3]{\xi_2 + \sqrt{\xi_2^2 - \xi_1^3}}} - \frac{1 \mp i\sqrt{3}}{2} \sqrt[3]{\xi_2 + \sqrt{\xi_2^2 - \xi_1^3}} \right), \quad (A1)$$

$$\lambda_3 = \frac{1}{3} \left( \alpha + \frac{\xi_1}{\sqrt[3]{\xi_2 + \sqrt{\xi_2^2 - \xi_1^3}}} + \sqrt[3]{\xi_2 + \sqrt{\xi_2^2 - \xi_1^3}} \right),$$

where  $\xi_1 = \alpha^2 + 3$ ,  $\xi_2 = \alpha^3 - 9\alpha + 27\beta^2$ , and  $\alpha = v_F/v_s$ , with  $\beta = v_c/v_s$ . These eigenvalues are important to get the renormalized spectrum of phonons and plasmons, collective excitations in the QH edge state (see Fig. 2 in the main text).

## APPENDIX B: CORRELATION FUNCTION AT ZERO TEMPERATURE

In this Appendix we calculate the correlation function of right-moving fermions  $G(x, t; x't')$  at filling factor  $\nu = 1$  in the presence of electron-phonon interaction at zero

temperature. Using the bosonization technique, we can write

$$G(x_1 t_1; x_2 t_2) \propto \langle e^{-i\hat{\phi}(x_1, t_1)} e^{i\hat{\phi}(x_2, t_2)} \rangle = e^{M(x_1 t_1; x_2 t_2)}, \quad (\text{B1})$$

where, in the Gaussian approximation and for equal bosonic autocorrelators, the function in the exponent is given by

$$M(x_1 t_1; x_2 t_2) = \langle \hat{\phi}(x_1, t_1) \hat{\phi}(x_2, t_2) \rangle - \langle \hat{\phi}^2(x_1, t_1) \rangle. \quad (\text{B2})$$

Next, using the definition of bosonic field in terms of creation and annihilation operators of bosons from Eq. (1), the cross correlator of bosonic fields takes the following form (zero modes are omitted):

$$\langle \hat{\phi}(x_1, t_1) \hat{\phi}(x_2, t_2) \rangle = \sum_{kk' > 0} \sqrt{\frac{(2\pi)^2}{kk' L^2}} [\langle \hat{a}_k(t_1) \hat{a}_{k'}^\dagger(t_2) \rangle e^{ikx_1 - ik'x_2} + \langle \hat{a}_k^\dagger(t_1) \hat{a}_{k'}(t_2) \rangle e^{-ikx_1 + ik'x_2}]. \quad (\text{B3})$$

Substituting the relation for bosonic operators in terms of BV-transformed new bosonic operators from Eq. (14),

$$\hat{a}_k(t) = b_{11} e^{-iv_1 kt} \hat{\alpha}_k(t) + b_{12} e^{-iv_2 kt} \hat{\beta}_k(t) + b_{13} e^{-iv_3 kt} \hat{\gamma}_{-k}^\dagger(t), \quad (\text{B4})$$

into the above cross correlator, we obtain the following simple combination of the sum of three terms:

$$M(x_1 t_1; x_2 t_2) = b_{11}^2 \mathcal{I}_1(x_1 t_1; x_2 t_2) + b_{12}^2 \mathcal{I}_2(x_1 t_1; x_2 t_2) + b_{13}^2 \mathcal{I}_3(x_1 t_1; x_2 t_2), \quad (\text{B5})$$

where

$$\begin{aligned} \mathcal{I}_1(x_1 t_1; x_2 t_2) &= \int_0^\infty dk \frac{e^{-\eta k}}{k} [e^{ik(x_1 - x_2) - iv_1 k(t_1 - t_2)} - 1] [1 + f_B^{(v_1)}(k)] + [e^{-ik(x_1 - x_2) + iv_1 k(t_1 - t_2)} - 1] f_B^{(v_1)}(k), \\ \mathcal{I}_2(x_1 t_1; x_2 t_2) &= \int_0^\infty dk \frac{e^{-\eta k}}{k} [e^{ik(x_1 - x_2) - iv_2 k(t_1 - t_2)} - 1] [1 + f_B^{(v_2)}(k)] + [e^{-ik(x_1 - x_2) + iv_2 k(t_1 - t_2)} - 1] f_B^{(v_2)}(k), \\ \mathcal{I}_3(x_1 t_1; x_2 t_2) &= \int_0^\infty dk \frac{e^{-\eta k}}{k} [e^{ik(x_1 - x_2) + iv_3 k(t_1 - t_2)} - 1] f_B^{(v_3)}(k) + [e^{-ik(x_1 - x_2) - iv_3 k(t_1 - t_2)} - 1] [1 + f_B^{(v_3)}(k)]. \end{aligned} \quad (\text{B6})$$

Here we introduced the new notations  $v_1 = \lambda_1 v_s$ ,  $v_2 = \lambda_2 v_s$ ,  $v_3 = -\lambda_3 v_s$ , where  $\lambda_i$ ,  $i = 1, 2, 3$ , are eigenvalues of the dynamical matrix;  $f_B^{(v_i)} = (e^{\beta v_i k} - 1)^{-1}$  is a bosonic distribution function,  $\beta$  is the inverse temperature, and  $i = 1, 2, 3$ . At zero temperature we have

$$\begin{aligned} \mathcal{I}_1(x_1 t_1; x_2 t_2) &= \int_0^\infty dk \frac{e^{-\eta k}}{k} [e^{ik(x_1 - x_2) - iv_1 k(t_1 - t_2)} - 1] = \ln \left[ \frac{\eta}{\eta - i[x_1 - x_2 - v_1(t_1 - t_2)]} \right], \\ \mathcal{I}_2(x_1 t_1; x_2 t_2) &= \int_0^\infty dk \frac{e^{-\eta k}}{k} [e^{ik(x_1 - x_2) - iv_2 k(t_1 - t_2)} - 1] = \ln \left[ \frac{\eta}{\eta - i[x_1 - x_2 - v_2(t_1 - t_2)]} \right], \\ \mathcal{I}_3(x_1 t_1; x_2 t_2) &= \int_0^\infty dk \frac{e^{-\eta k}}{k} [e^{-ik(x_1 - x_2) - iv_3 k(t_1 - t_2)} - 1] = \ln \left[ \frac{\eta}{\eta + i[x_1 - x_2 + v_3(t_1 - t_2)]} \right]. \end{aligned} \quad (\text{B7})$$

Substituting Eq. (B7) into Eq. (B5) and then into Eq. (B1), we finally get the expression for the two-point correlation function in the form

$$G(x_1, t_1; x_2, t_2) \propto \left[ \frac{i\eta}{x_1 - x_2 - v_1(t_1 - t_2) + i\eta} \right]^{b_{11}^2} \left[ \frac{i\eta}{x_1 - x_2 - v_2(t_1 - t_2) + i\eta} \right]^{b_{12}^2} \left[ \frac{-i\eta}{x_1 - x_2 + v_3(t_1 - t_2) - i\eta} \right]^{b_{13}^2}. \quad (\text{B8})$$

### APPENDIX C: THERMAL HALL CONDUCTANCE

Here we calculate the thermal Hall conductance of the chiral edge channel coupled to acoustic phonons. According to Eqs. (15) and (16) of THE main text there are three modes which propagate with velocities  $v_i$ ,  $i = 1, 2, 3$ , in the  $\chi_i = \pm 1$  direction. The dispersion relation is given by Eq. (13) of the main text and has the linear form  $\epsilon_i(k) = v_i k$ . At temperature  $T$ , each mode is characterized by the equilibrium bosonic distribution function  $f_B^{(v_i)}(k) = (e^{v_i k/T} - 1)^{-1}$ . Thus, the thermal current is given by [31]

$$I_Q = \sum_{i=1}^3 \chi_i v_i n_{Q_i}, \quad (\text{C1})$$

where the energy density of mode  $i$  (restoring natural units)

can be expressed as [31]

$$n_{Q_i} = \int \frac{dk}{2\pi} \epsilon_i(k) f_B^{(v_i)}(k) = \frac{1}{v_i} \frac{\pi^2}{6} \frac{k_B^2}{h} T^2. \quad (\text{C2})$$

The thermal Hall conductance is evaluated as the derivative of the current with respect to temperature [31], namely,

$$K_H = \frac{\partial I_Q}{\partial T} = \chi_Q \frac{\pi^2}{3} \frac{k_B^2}{h} T, \quad (\text{C3})$$

where the prefactor  $\chi_Q = \sum_i \chi_i = 1$  is the difference between the number of upstream and downstream modes. Therefore, the thermal  $K_H$  and electrical  $G_H = e^2/h$  Hall conductances are related by the Wiedemann-Franz law as in the case of free electrons. Namely,  $K_H/G_H = TL_0$ , where  $L_0 = (\pi^3/3)(k_B/e)^2$  is a free-electron Lorenz number.

- [1] J. Bardeen, L. N. Cooper, and J. R. Schrieffer, *Phys. Rev.* **106**, 162 (1957).
- [2] J. Bardeen, L. N. Cooper, and J. R. Schrieffer, *Phys. Rev.* **108**, 1175 (1957).
- [3] D. Loss and T. Martin, *Phys. Rev. B* **50**, 12160 (1994).
- [4] T. Martin and D. Loss, *Int. J. Mod. Phys. B* **09**, 495 (1995).
- [5] P. Kopietz, *Z. Phys. B* **100**, 561 (1996).
- [6] T. Brandes and A. Kawabata, *Phys. Rev. B* **54**, 4444 (1996).
- [7] C. S. Rao, P. M. Krishna, S. Mukhopadhyay and A. Chatterjee, *J. Phys.: Condens. Matter* **13**, L919 (2001).
- [8] W. Izumida and M. Grifoni, *New J. Phys.* **7**, 244 (2005).
- [9] T. L. Schmidt, *Phys. Rev. Lett.* **107**, 096602 (2011).
- [10] A. Galda, I. V. Yurkevich, and I. V. Lerner, *Phys. Rev. B* **83**, 041106(R) (2011).
- [11] A. Galda, I. V. Yurkevich, and I. V. Lerner, *Europhys. Lett.* **93**, 17009 (2011).
- [12] I. V. Yurkevich, A. Galda, O. M. Yevtushenko, and I. V. Lerner, *Phys. Rev. Lett.* **110**, 136405 (2013).
- [13] S. Groenendijk, G. Dolcetto, and T. L. Schmidt, *Phys. Rev. B* **97**, 241406(R) (2018).
- [14] G. Wentzel, *Phys. Rev.* **83**, 168 (1951).
- [15] J. Bardeen, *Rev. Mod. Phys.* **23**, 261 (1951).
- [16] I. V. Yurkevich, *Europhys. Lett.* **104**, 37004 (2013).
- [17] I. V. Yurkevich and O. M. Yevtushenko, *Phys. Rev. B* **90**, 115411 (2014).
- [18] Z. F. Ezawa, *Quantum Hall Effects: Recent Theoretical and Experimental Developments*, 3rd ed. (World Scientific, Singapore, 2013).
- [19] K. v. Klitzing, G. Dorda, and M. Pepper, *Phys. Rev. Lett.* **45**, 494 (1980).
- [20] D. C. Tsui, H. L. Stormer, and A. C. Gossard, *Phys. Rev. Lett.* **48**, 1559 (1982).
- [21] X. G. Wen, *Adv. Phys.* **44**, 405 (1995).
- [22] Edited by B. Douçot, V. Pasquier, B. Duplantier, and V. Rivasseau, *The Quantum Hall Effect*, Progress in Mathematical Physics, Vol. 45 (Birkhäuser, Basel, 2005).
- [23] X. G. Wen, *Phys. Rev. B* **41**, 12838 (1990).
- [24] C. de C. Chamon, D. E. Freed, and X. G. Wen, *Phys. Rev. B* **51**, 2363 (1995).
- [25] C. de C. Chamon, D. E. Freed, and X. G. Wen, *Phys. Rev. B* **53**, 4033 (1996).
- [26] C. de C. Chamon, D. E. Freed, S. A. Kivelson, S. L. Sondhi, and X. G. Wen, *Phys. Rev. B* **55**, 2331 (1997).
- [27] A. Crépieux, P. Devillard, and T. Martin, *Phys. Rev. B* **69**, 205302 (2004).
- [28] C. de C. Chamon and X. G. Wen, *Phys. Rev. Lett.* **70**, 2605 (1993).
- [29] O. Heinonen and S. Eggert, *Phys. Rev. Lett.* **77**, 358 (1996).
- [30] C. L. Kane and M. P. A. Fisher, *Phys. Rev. Lett.* **76**, 3192 (1996).
- [31] C. L. Kane and M. P. A. Fisher, *Phys. Rev. B* **55**, 15832 (1997).
- [32] C. Grenier, R. Hervé, G. Fevè, and P. Degiovanni, *Mod. Phys. Lett. B* **25**, 1053 (2011).
- [33] F. P. Milliken, C. P. Umbach, and R. A. Webb, *Solid State Commun.* **97**, 309 (1996).
- [34] D. B. Chklovskii, B. I. Shklovskii, and L. I. Glazman, *Phys. Rev. B* **46**, 4026 (1992).
- [35] M. Xiao, [arXiv:0908.0787](https://arxiv.org/abs/0908.0787).
- [36] *Bosonization and Strongly Correlated Systems*, edited by A. O. Gogolin, A. A. Nersesyan, and A. M. Tsvelik (Cambridge University Press, Cambridge, 2004).
- [37] A. O. Slobodeniuk, E. G. Idrisov, and E. V. Sukhorukov, *Phys. Rev. B* **93**, 035421 (2016).
- [38] E. G. Idrisov, I. P. Levkivskiy, and E. V. Sukhorukov, *Phys. Rev. Lett.* **121**, 026802 (2018).
- [39] D. C. Glatli, Tunneling experiments in the fractional Quantum Hall effect regime, in *The Quantum Hall Effect*, Progress in Mathematical Physics, Vol. 45, edited by B. Douçot, V. Pasquier, B. Duplantier, V. Rivasseau (Birkhäuser, Basel, 2005).
- [40] G. B. Lesovik and R. Loosen, *JETP Lett.* **65**, 295 (1997).
- [41] J. Basset, H. Bouchiat, and R. Deblock, *Phys. Rev. Lett.* **105**, 166801 (2010).
- [42] J. Dubois, T. Jullien, F. Portier, P. Roche, A. Cavanna, Y. Jin, W. Wegscheider, P. Roulleau, and C. Glatli, *Nature (London)* **502**, 659 (2013).
- [43] P. P. Hofer and C. Flindt, *Phys. Rev. B* **90**, 235416 (2014).
- [44] J. Rech, D. Ferraro, T. Jonckheere, L. Vannucci, M. Sassetti, and T. Martin, *Phys. Rev. Lett.* **118**, 076801 (2017).
- [45] C. Glatli and P. Roulleau, *Phys. Status Solidi B* **254**, 1600650 (2017).
- [46] M. Kapfer, P. Roulleau, M. Santin, I. Farrer, D. A. Ritchie, and D. C. Glatli, *Science* **363**, 846 (2019).